

Supporting Information

Assigning the EPR Fine Structure Parameters of the Mn(II) Centers in *Bacillus subtilis* Oxalate Decarboxylase by Site-Directed Mutagenesis and DFT/MM Calculations

Pablo Campomanes, Whitney F. Kellett, Lindsey M. Easton, Andrew Ozarowski, Karen N. Allen,
Alexander Angerhofer, Ursula Rothlisberger, and Nigel G. J. Richards

Laboratory of Computational Chemistry and Biochemistry, Federal Institute of Technology, EPFL, CH-1015 Lausanne, Switzerland, the Department of Chemistry & Chemical Biology, Indiana University Purdue University Indianapolis, Indianapolis, IN 46202, United States, the Department of Chemistry, Boston University, Boston, MA 32310, United States, the Department of Chemistry, University of Florida, Gainesville, FL 32611, United States, and the National High Magnetic Field Laboratory, Florida State University, Tallahassee, FL 32310, United States

Table S1. EPR zfs parameters for C-terminally His₆-tagged, WT OxDC and the Mn(II)-containing W132F OxDC variant at pH 8.5.^a *D* and *E* are obtained from low-resolution spectra (3 K) while *g* and *A* are obtained from high-resolution spectra.

	<i>D</i> (MHz)	<i>E/D</i>	<i>g</i>	<i>A</i> _{iso} (MHz)	Linewidth (G)	Weight (%)
WT OxDC site I	-1350	0.15	2.00089	251.3	6	68
WT OxDC site II	10430	0.20	2.00080	250.0	4	32
W132F site I	-1950	0.21	2.00089	251.3	6	69
W132F site II	10430	0.20	2.00080	250.0	4	31

^a Other EasySpin¹ simulation parameters used to obtain EPR zfs values:

(1) WT OxDC (site I): Hstrain_{iso} = 20 MHz, *E* = 200 MHz, Dstrain = 0.4×|*D*|, Estrain = 4×|*E*|

(2) WT OxDC (site II): Hstrain_{iso} = none, *E* = 2100 MHz, Dstrain = 0.1×|*D*|, Estrain = 0.1×|*E*|

(3) W132F (site I): Hstrain_{iso} = 60 MHz, *E* = 400 MHz, Dstrain = 0.4×|*D*|, Estrain = 2×|*E*|

(4) W132F (site II): Hstrain_{iso} = none, *E* = 2100 MHz, Dstrain = 0.1×|*D*|, Estrain = 0.1×|*E*|

Table S2. Fine structure parameters, D and E (MHz), of the Mn(II) binding sites in WT OxDC and the Mn-containing W132F OxDC variant calculated using both the hybrid B3LYP² and the non-hybrid BP86³ functional in conjunction with double-zeta⁴ (SVP) and triple-zeta⁵ (TZVP) basis sets. The spin-spin (SSC) and spin-orbit (SOC) contributions to D and E are also reported (MHz).

	<i>Theory Level</i>	D	E/D	D (SSC)	E (SSC)	D (SOC)	E (SOC)
WT OxDC (N-Term)	B3LYP/TZVP	-1170	0.11	240	90	-1410	-220
WT OxDC (N-Term)	B3LYP/SVP	920	0.09	-490	-10	1410	90
WT OxDC (N-Term)	BP86/TZVP	1100	0.17	-520	130	1620	60
WT OxDC (N-Term)	BP86/SVP	1010	0.21	-550	120	1560	90
WT OxDC (C-Term) ^a	B3LYP/TZVP	-7130	0.13	-60	-620	-7070	-300
WT OxDC (C-Term) ^a	B3LYP/SVP	-3780	0.18	-100	-510	-3680	-160
WT OxDC (C-Term) ^a	BP86/TZVP	-3290	0.19	-80	-310	-3210	-300
WT OxDC (C-Term) ^a	BP86/SVP	-2850	0.23	-150	-440	-2700	-210
W132F (N-Term) ^b	B3LYP/TZVP	-2100	0.23	620	160	-2720	-650
W132F (N-Term) ^b	B3LYP/SVP	-1340	0.29	610	210	-1950	-600
W132F (N-Term) ^b	BP86/SVP	1130	0.24	-660	-230	1790	500
W132F (N-Term) ^c	B3LYP/TZVP	-1350	0.10	210	250	-1560	-390
W132F (N-Term) ^c	B3LYP/SVP	1190	0.11	-530	70	1720	60
W132F (N-Term) ^c	BP86/SVP	1310	0.15	-580	130	1890	60

^a Cluster model containing hydroxide as the fifth ligand with a hydrogen bond to a solvent water (Figure 7d in main text). ^b Initial structure for QM/MM optimization based on the X-ray crystal structure of Co(II)-containing W132F OxDC variant. ^c Initial structure for QM/MM optimization from *in silico* modification of the X-ray crystal structure of WT OxDC (1UW8).

Figure S1. Simulated powder EPR spectra of the lowest energy transition $|-5/2\rangle \leftrightarrow |-3/2\rangle$ when $D = -3500$ MHz (black) and $D = +3500$ MHz (red) at 326.4 GHz assuming $E = 500$ MHz. These simulations illustrate how the sign of D can be extracted from the shape of the EPR spectrum at very low temperatures where only the lowest spin state has appreciable Boltzmann population.

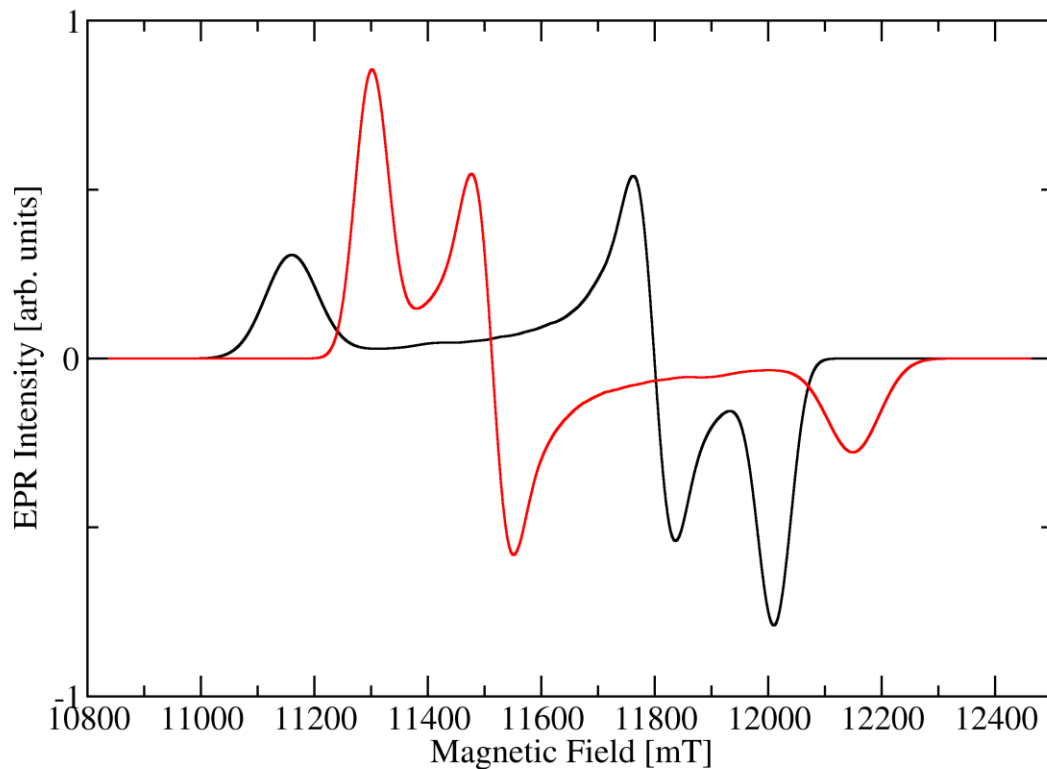


Figure S2. Simulated EPR spectra of the central sextet transition $|-1/2\rangle \leftrightarrow |+1/2\rangle$ when $|D| = 1200$ MHz and $|E| = 200$ MHz (black), $|D| = 4100$ MHz and $|E| = 1000$ MHz (red) and $|D| = 10600$ MHz and $|E| = 2000$ MHz (green) at 326.4 GHz. This graph illustrates how the magnitude of the zero field splitting affects the shape of the central sextet. When there is spectral overlap between Mn(II) sites of variable size of D , the site with the largest D tends to have a weaker and more spread-out spectrum. In the case of OxDC it can usually only be recognized by a few of the low-field peaks and the Pake pattern at high fields. Since the effect of D on the lineshape is of second order, i.e., dependent on the square, the sign of D cannot be extracted from the spectrum.

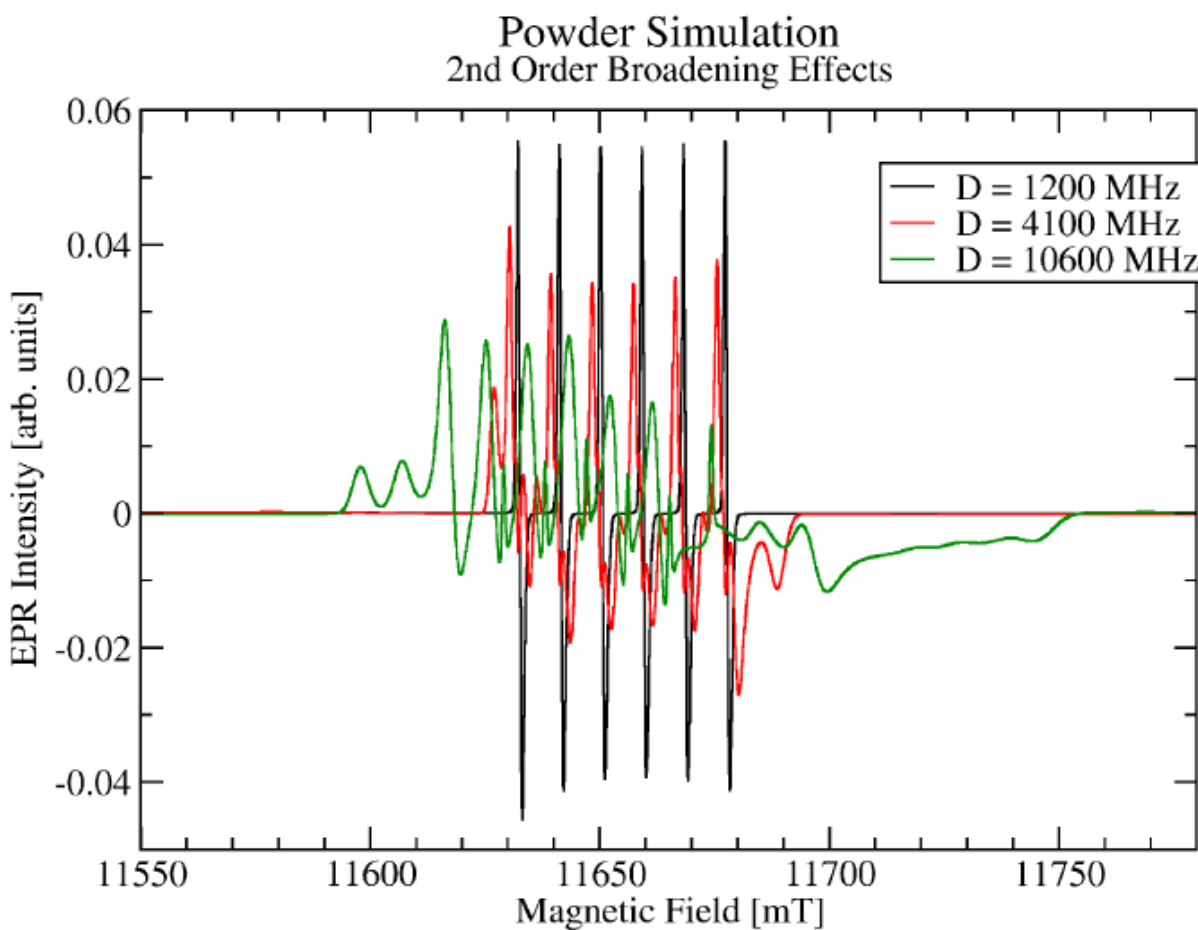


Figure S3. High-field (326.4 GHz) EPR spectra of WT O_xDC taken at 3 K (blue) together with spectral simulations. The field modulation amplitude was 19.5 G and the sweep speed 2 mT/s. The sample temperature was set to 3 K. Lines from spectral simulations correspond to a single Mn(II) species (site I) (green) and a single Mn(II) species (site II) (cyan). The sum of site I and site II simulations is also shown (red). The simulation parameters are the same as those given in Figure 2 (main text).

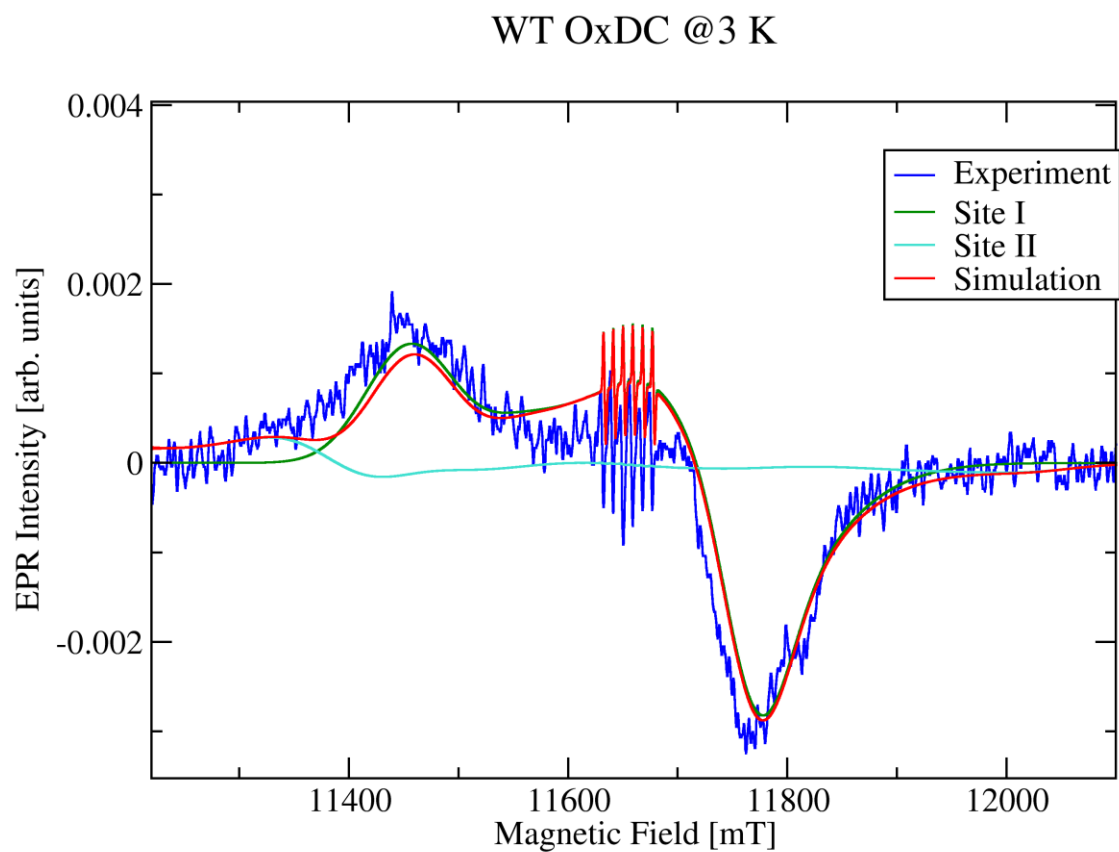


Figure S4. High-field (326.4 GHz) EPR spectra of WT OxDC taken at 40K (blue) together with spectral simulations. The spectrum depicts primarily the central sextet lines and their simulations. The field modulation amplitude was 19.5 G and the sweep speed 2 mT/s. Sample temperature was set to 40 K. Lines from spectral simulations correspond to a single Mn(II) species (site I) (green) and a single Mn(II) species (site II) (cyan). The sum of site I and site II simulations is also shown (red). The simulation parameters are the same as those given in Figure 2 (main text).

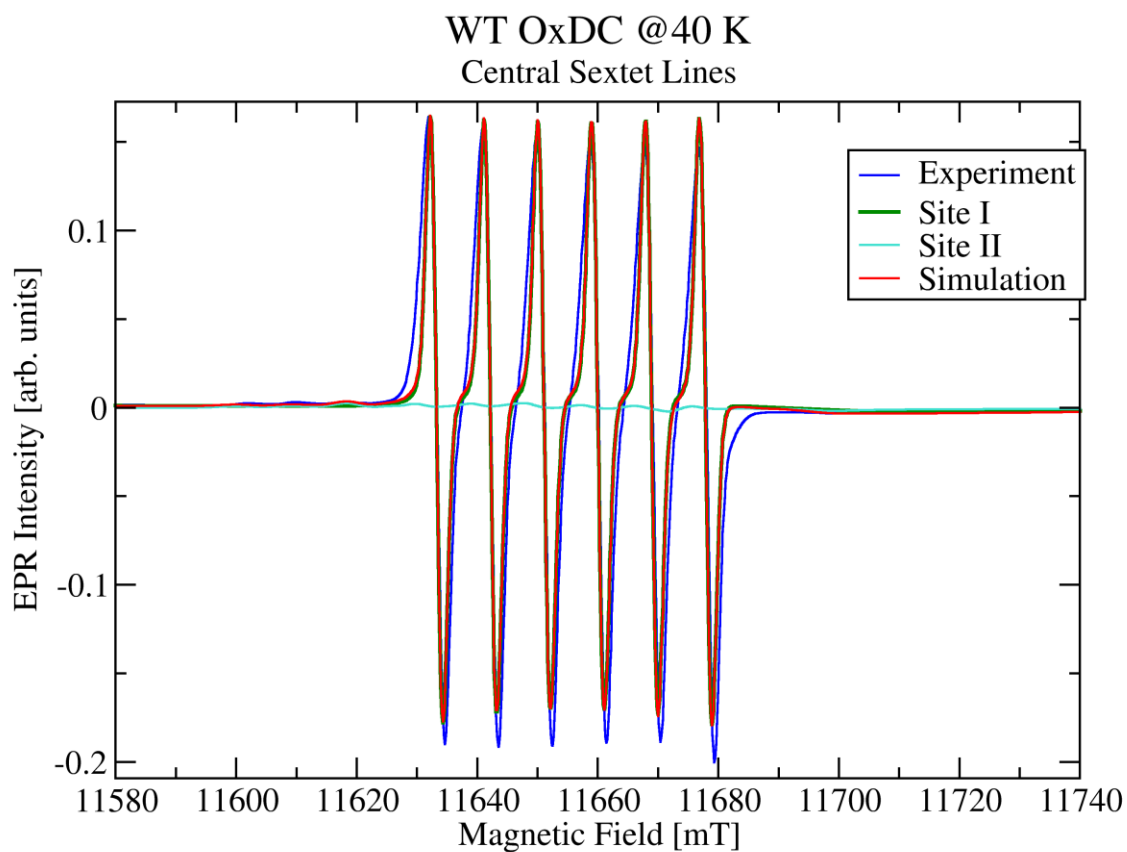


Figure S5. Michaelis-Menten plot used to obtain the steady-state kinetic parameters. Error bars represent the standard error of three independent measurements. Reaction mixtures consisted of enzyme (15 μg) and potassium oxalate (2 – 100 mM) dissolved in 50 mM NaOAc, pH 4.2, containing 0.5 mM *o*-phenylenediamine and 0.2% Triton-X100 (100 μL total volume). Turnover was initiated by the addition of enzyme. After incubation at 25 $^{\circ}\text{C}$, the reaction was quenched by the addition of 1.0 M aq. NaOH (10 μL), and the formate quantified using the NADH absorption at 340 nm in an assay mixture containing formate dehydrogenase.⁶

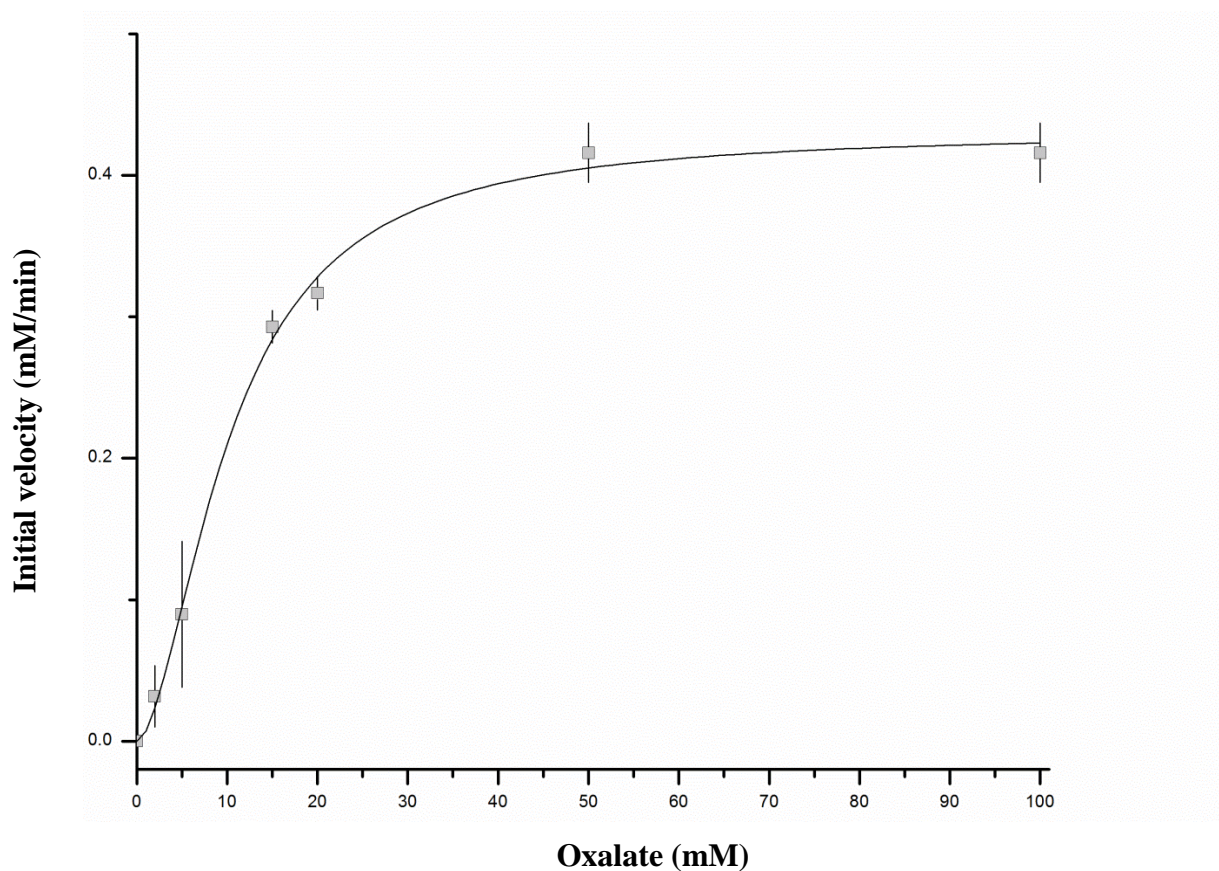


Figure S6. The active site of the Co(II)-containing W132F OxDC variant. Protein residues are rendered in stick representation with waters (red) and the cobalt ion (pink) shown as spheres. Ligand-metal coordinate bond lengths (dotted lines) are labeled in black and pink for the Co(II)-containing W132F OxDC variant and Mn(II)-containing WT OxDC (1UW8), respectively.

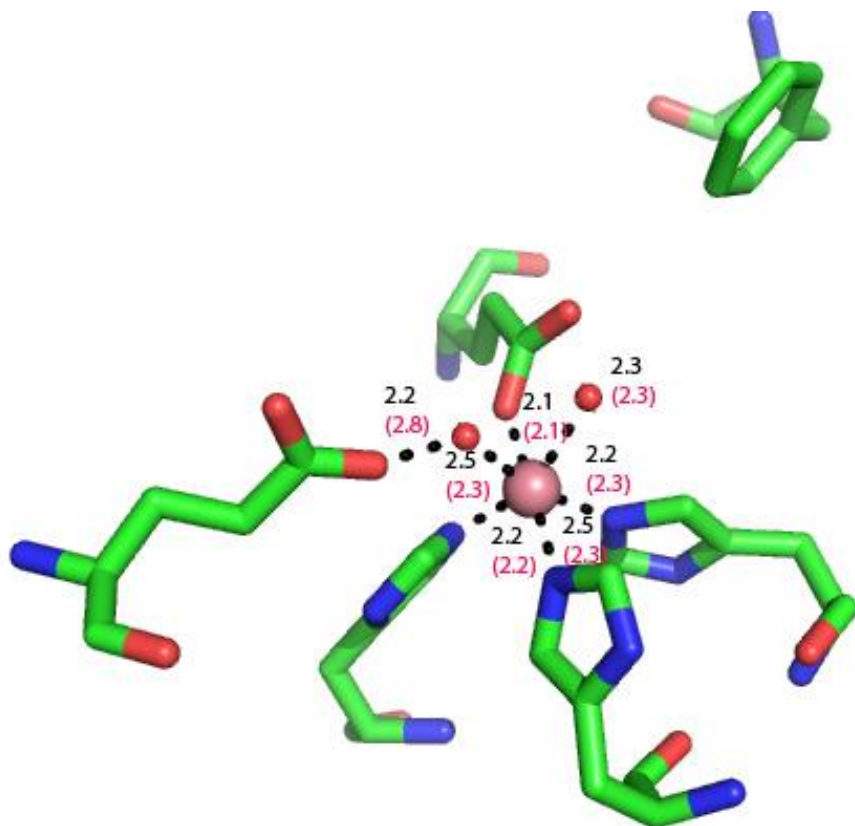
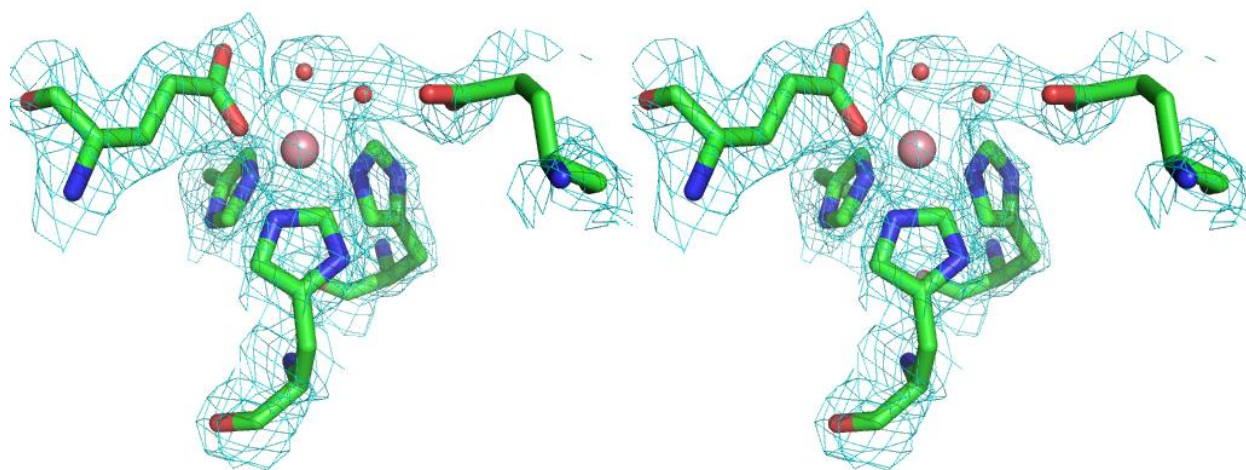


Figure S7. (A) Stereo view of the active site of the Co-containing W132F OxDC variant showing the simulated-annealing composite omit electron density map calculated with coefficients $2F_o - F_c$ and contoured at $d > 2\sigma$ (cyan cages). (B) Same structure rotated by 90° about the x-, y-, and z-axes. In both figures, protein residues are rendered in stick representation with waters (red) and the cobalt ion (pink) shown as spheres.

(A)



(B)

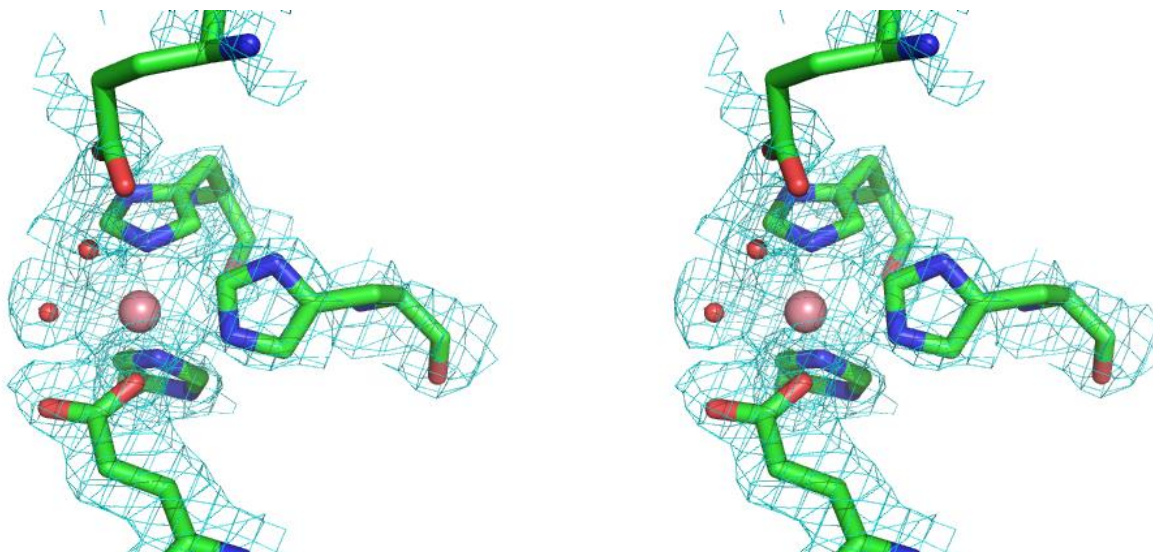


Figure S8. High-field (326.4 GHz) EPR spectra of the Mn-containing W132F O_xDC variant taken at 3 K (blue) together with spectral simulations. The field modulation amplitude was 20 G and the sweep speed 2 mT/s. Sample temperature was set to 3 K. Lines from spectral simulations correspond to a single Mn(II) species (N terminal site I) (green) and a single Mn(II) species (C-terminal site II) (cyan). The sum of site I and site II simulations is also shown (red). The simulation parameters are the same as those given in Figure 6 (main text).

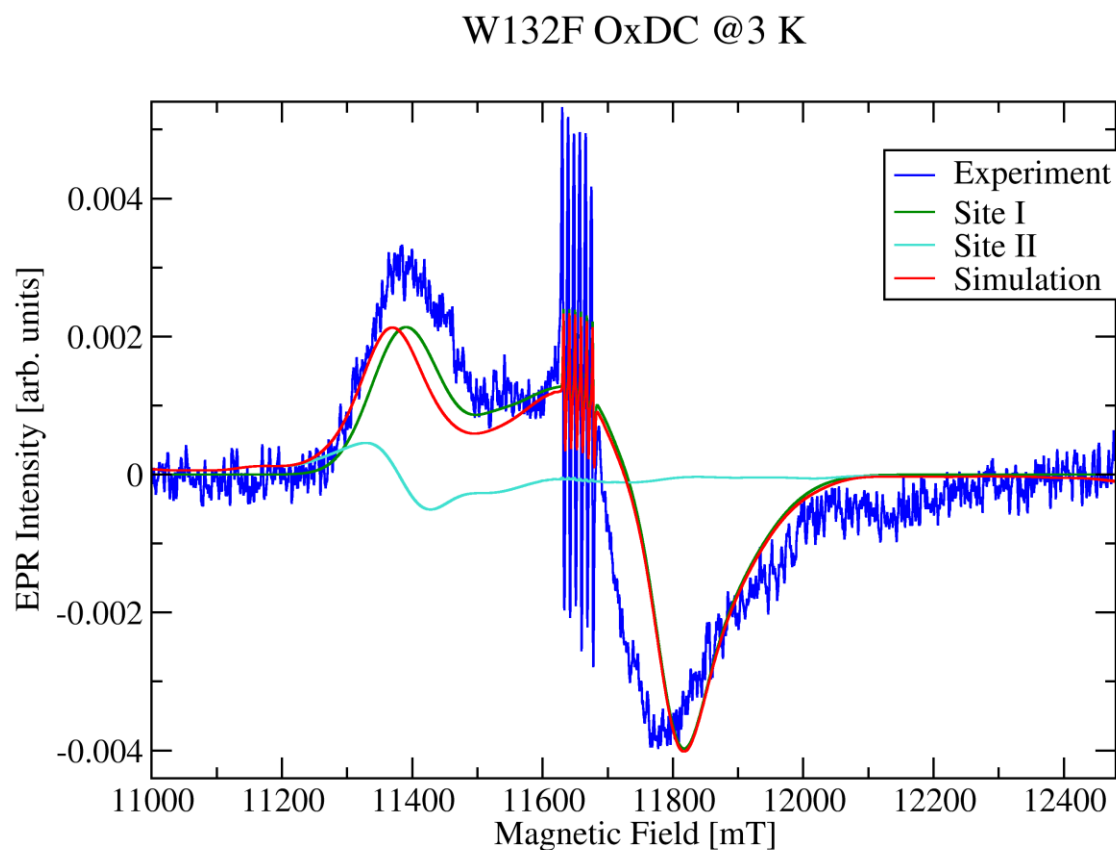


Figure S9. High-field (326.4 GHz) EPR spectra of the Mn-containing W132F OxDc variant taken at 40K (blue) together with spectral simulations. The spectrum depicts primarily the central sextet lines and their simulations. The field modulation amplitude was 19.5 G and the sweep speed 2 mT/s. Sample temperature was set to 40 K. Lines from spectral simulations correspond to a single Mn(II) species (N terminal site I) (green) and a single Mn(II) species (C-terminal site II) (cyan). The sum of site I and site II simulations is also shown (red). The simulation parameters are the same as those given in Figure 6 (main text).

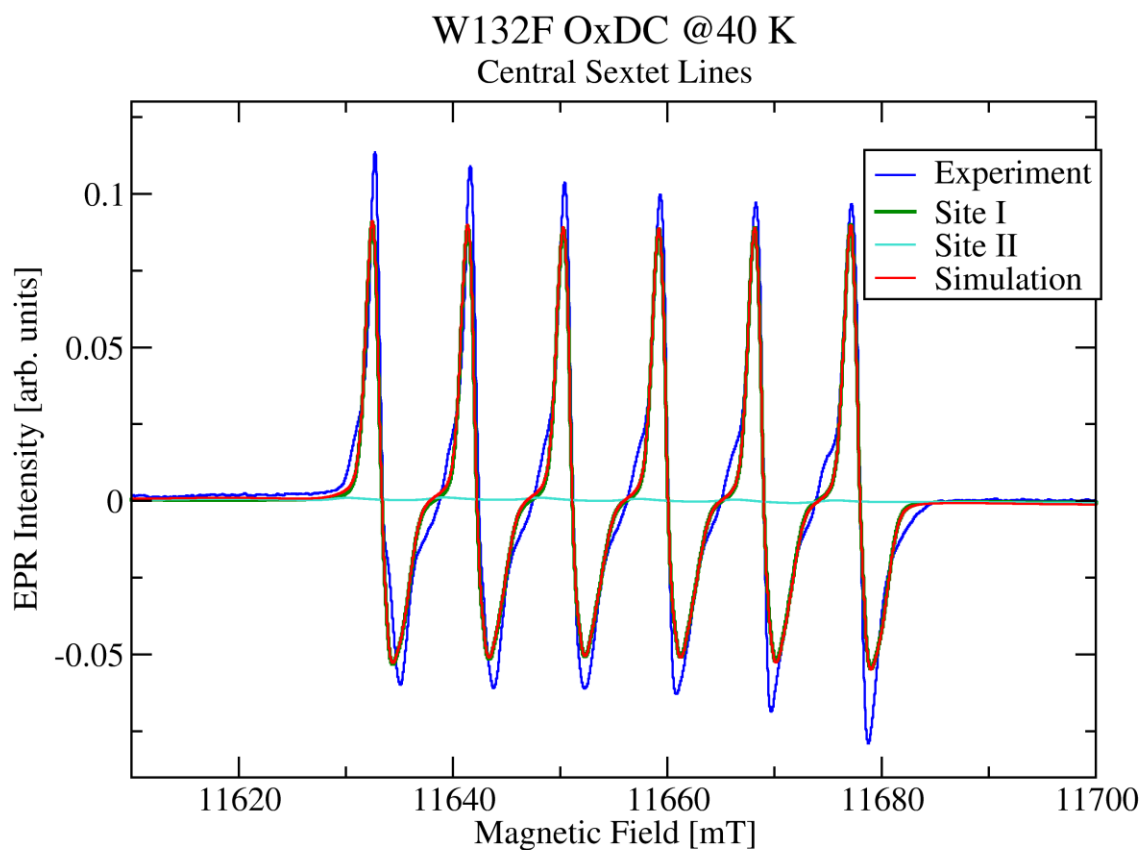
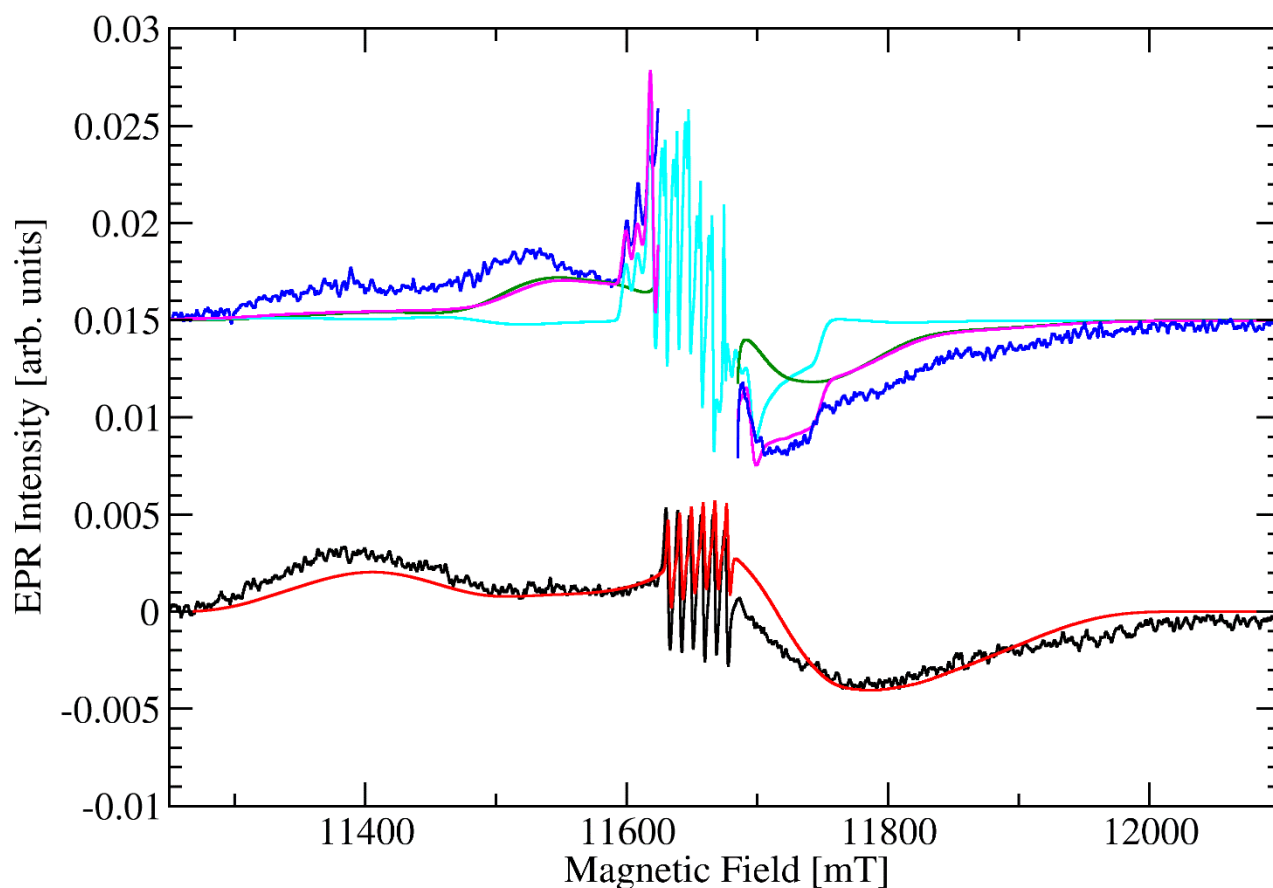


Figure S10. High-field (326.4 GHz) EPR spectra of the Mn-containing W132F OxDC variant taken at 3K (black) and 40K (blue) together with spectral simulations. Note that the central part of the spectrum at 40 K together with the corresponding spectral simulation of site I is removed for clarity. The enzyme (40 mg/mL) was dissolved in 50 mM Tris buffer containing 500 mM NaCl, pH 8.5. Lines from spectral simulations correspond to a single Mn(II) species (site I) with small zfs at 3 K (red) and 40 K (green), and a single Mn(II) species (site II) with very large zfs at 40 K (cyan). The sum of site I and site II simulations at 40 K is also shown (magenta). In this case, however, a broad non-Gaussian spectral distribution of zfs values was assumed ranging from $D = -1600$ MHz through $D = -2100$ MHz and from $E = 100$ MHz through $E = |D|/3$.



Overlap extension mutagenesis and plasmid purification. The gene encoding the W132F OxDC variant was constructed using the overlap extension method⁷ with the following primers:

OxDC (NdeI):

Forward: 5' – GGAGGAAACATCATATGAAAAAACA – 3'

OxDC (XhoI):

Reverse: 5' – GTGGTGCTCGAGTTTACTGCATTTTC – 3'

W132F:

Forward: 5' – GGTGAAGGAGACCTTTTCTACTTCCC – 3'

Reverse: 5' – GGCAGGCCTGACGGGAAGTAGAAA – 3'

Briefly, polymerase chain reactions (PCRs) were conducted in solutions containing 40 μ L H₂O, 5 μ L of *PfuTurbo* AD 10x buffer, 50 ng of template OxDC in pET32a, 0.25 mM dNTP mixture, 0.2 μ M of forward primer, 0.2 μ M of reverse primer, 1 μ L of *PfuTurbo* AD enzyme (50 μ L total volume). The first set of PCRs were run for four minutes at 95 °C followed by 30 cycles of denaturing at 95 °C for 30 s, annealing at 55 °C for 1 min, and extension at 72 °C for 7 min. After a final extension phase at 72 °C for 10 min, the solution was cooled to 4 °C. A second set of PCRs to stitch together PCR products from the first round were then performed using solutions containing 40 μ L H₂O, 5 μ L *PfuTurbo* AD 10x buffer, 1 μ L of each of the first round PCR mixtures, 0.2 mM dNTP mixture, 0.2 μ M of OxDC forward *NdeI* primer, 0.2 μ M OxDC *XhoI* reverse primer, and 1 μ L *PfuTurbo* AD enzyme (50 μ L total volume). After following an identical set of denaturing, annealing and extension cycles to those used in the first round of PCRs, DNA was purified using a Wizard kit (Promega). The purified DNA was cut at 37 °C for 1-2 hours using the *XhoI* and *NdeI* restriction enzymes (New England Biolabs) and ligated into pET32a (Novagen), which had been cut previously with *NdeI* and *XhoI* and treated with calf intestinal alkaline phosphatase. Ligation with T4 DNA ligase (New England Biolabs) was performed at 16° C for 16 hours. JM109 cells were transformed with the ligation mixture (1-5 μ L), plated on Luria broth with 0.1 mg/mL ampicillin and grown overnight at 37 °C. The resulting colonies were grown overnight at 37 °C in LBA (50 mL) and plasmids purified using a Wizard kit (Promega). DNA sequencing was then performed to ensure that the correct mutation had been introduced into the gene (Interdisciplinary Center for Biotechnology Research at the University of Florida).

Literature Cited

1. Stoll, S.; Schweiger, A. *J. Magn. Reson.* **2006**, *178*, 42-55.
2. Becke, A. D. *J. Chem. Phys.* **1993**, *98*, 1372-1377.
3. (a) Becke, A. D. *Phys. Rev. A* **1988**, *38*, 3098-3100. (b) Perdew, J. P. *Phys. Rev. B* **1986**, *33*, 8822-8824.
4. Schäfer, A.; Horn, H.; Ahlrichs, R. *J. Chem. Phys.* **1992**, *97*, 2571-2577.
5. Weigend, F.; Ahlrichs, R. *Phys. Chem. Chem. Phys.* **2005**, *7*, 3297-3305.
6. Schutte, H.; Flossdorf, J.; Sahm, H.; Kula, M. R. *Eur. J. Biochem.* **1976**, *62*, 152-160.
7. Ho, S. N.; Hunt, H. D.; Horton, R. M.; Pullen, J. K.; Lease, L. R. *Gene* **1989**, *77*, 51-59.

Cartesian coordinates for the cluster models used to calculate zfs parameters (numbers refer to figures in the main text).

(A) WT OxDC (N-terminal Mn(II) site; Figure 7a) $D = -1170$ MHz, $E/D = 0.11$:

H	-1.430	4.017	5.967
C	-2.184	3.414	5.446
H	-2.446	2.579	6.101
H	-3.083	4.032	5.325
C	-1.685	2.895	4.143
N	-1.187	3.703	3.133
H	-1.094	4.709	3.171
C	-0.831	2.910	2.087
H	-0.392	3.281	1.172
N	-1.077	1.645	2.363
C	-1.601	1.624	3.640
H	-1.855	0.697	4.130
H	-4.969	-3.433	4.496
C	-5.164	-2.836	3.597
H	-5.886	-3.383	2.979
H	-5.642	-1.905	3.914
C	-3.901	-2.528	2.856
N	-3.117	-3.494	2.241
H	-3.365	-4.468	2.136
C	-2.032	-2.888	1.691
H	-1.257	-3.398	1.139
N	-2.062	-1.588	1.923
C	-3.224	-1.356	2.638
H	-3.507	-0.360	2.943
H	1.585	-5.397	-0.762
C	1.153	-4.439	-0.451
H	0.123	-4.402	-0.821
H	1.123	-4.421	0.644
C	1.972	-3.279	-1.007
H	3.024	-3.376	-0.714
H	1.969	-3.301	-2.105
C	1.517	-1.881	-0.588
O	0.384	-1.767	0.000
O	2.290	-0.924	-0.858
H	3.654	0.100	6.278
C	3.872	-0.131	5.229
H	4.387	0.729	4.795
H	4.570	-0.977	5.200
C	2.625	-0.424	4.452
N	1.709	-1.381	4.863
H	1.784	-1.936	5.702
C	0.707	-1.454	3.947
H	-0.139	-2.115	4.066
N	0.919	-0.595	2.965
C	2.107	0.050	3.271

H	2.510	0.804	2.611
Mn	-0.453	-0.154	1.099
O	-0.196	3.100	-1.523
H	0.157	3.000	-2.421
H	-1.175	2.947	-1.608
O	-2.120	0.558	-0.369
H	-2.442	0.047	-1.133
H	-2.351	1.482	-0.628
O	1.019	1.184	0.148
H	1.587	0.504	-0.328
H	0.633	1.791	-0.527

(B) WT OxDC (C-terminal Mn(II) site; Figure 7d) D = -7130 MHz, E/D = 0.13:

H	12.411	6.938	14.520
C	12.683	7.667	15.269
H	11.822	7.838	15.922
H	13.475	7.236	15.891
C	13.090	8.976	14.671
N	14.350	9.233	14.141
H	15.146	8.585	14.112
C	14.353	10.522	13.682
H	15.207	11.017	13.250
N	13.168	11.097	13.869
C	12.376	10.139	14.483
H	11.352	10.338	14.758
H	6.934	11.715	14.408
C	7.121	12.735	14.108
H	6.780	12.841	13.073
H	6.519	13.407	14.732
C	8.582	13.033	14.221
N	9.231	13.207	15.442
H	8.778	13.298	16.357
C	10.572	13.329	15.195
H	11.325	13.479	15.953
N	10.816	13.237	13.890
C	9.580	13.064	13.277
H	9.471	12.985	12.208
H	9.538	17.271	10.213
C	10.263	16.516	10.479
H	9.817	15.902	11.266
H	10.428	15.880	9.600
C	11.607	17.112	10.977
H	12.109	17.695	10.201
H	11.418	17.807	11.807
C	12.617	16.067	11.491
O	12.100	15.102	12.186
O	13.849	16.213	11.250
H	13.676	8.434	8.727
C	13.543	9.449	8.382

H	14.507	9.839	8.039
H	12.902	9.385	7.494
C	12.963	10.370	9.410
N	11.605	10.377	9.735
H	10.853	9.859	9.270
C	11.403	11.348	10.674
H	10.421	11.549	11.066
N	12.543	11.963	10.985
C	13.519	11.354	10.197
H	14.548	11.678	10.238
Mn	12.894	13.355	12.919
O	14.824	13.420	13.445
H	15.287	14.264	13.294
O	13.732	13.683	15.813
H	14.286	13.512	14.963
H	13.947	14.617	16.036

(C) W132F OxDC variant (N-terminal Mn(II) site; initial structure based on the X-ray crystal structure of the Co(II)-containing variant) D = -2100 MHz, E/D = 0.23:

C	16.601	12.822	11.771
C	17.488	12.230	10.899
N	17.461	10.879	11.242
C	16.587	10.708	12.279
N	16.049	11.874	12.640
C	18.333	12.741	9.765
Mn	14.754	12.337	14.555
O	14.017	14.265	13.588
N	16.643	13.313	15.244
C	17.263	14.285	14.571
N	18.585	14.314	14.884
C	18.844	13.307	15.811
C	17.626	12.705	16.022
C	20.196	12.994	16.377
N	15.083	10.538	15.842
C	14.296	10.130	16.838
N	14.389	8.773	16.989
C	15.272	8.289	16.024
C	15.693	9.397	15.339
C	15.514	6.840	15.773
O	13.181	11.234	13.593
C	12.180	11.749	12.939
O	11.865	12.978	12.955
C	11.334	10.790	12.104
C	10.251	10.089	12.968
O	13.500	13.217	16.390
H	20.866	12.543	15.660
H	20.064	12.304	17.215
H	20.698	13.887	16.763
H	19.266	14.926	14.446

H	16.802	14.952	13.861
H	17.397	11.869	16.663
H	16.475	6.480	16.109
H	15.445	6.646	14.695
H	14.728	6.253	16.254
H	13.909	8.221	17.694
H	13.654	10.760	17.427
H	16.369	9.440	14.504
H	9.700	9.324	12.441
H	9.530	10.828	13.335
H	10.693	9.615	13.849
H	11.994	10.047	11.644
H	10.870	11.375	11.305
H	19.340	13.017	10.041
H	17.852	13.599	9.283
H	18.448	11.967	8.998
H	18.036	10.149	10.835
H	16.343	9.732	12.662
H	16.303	13.857	11.814
H	12.551	13.285	16.185
H	13.578	13.613	17.324
H	13.100	13.877	13.308
H	13.815	14.928	14.271

(D) W132F OxDC variant (N-terminal Mn(II) site; initial structure derived from the X-ray crystal structure of WT OxDC (*in silico* substitution)) D = -1350 MHz, E/D = 0.10:

H	-1.239	4.539	5.523
C	-1.951	3.804	5.126
H	-2.074	3.027	5.885
H	-2.921	4.307	5.010
C	-1.483	3.199	3.854
N	-1.144	3.939	2.733
H	-1.175	4.947	2.659
C	-0.775	3.077	1.749
H	-0.438	3.386	0.771
N	-0.862	1.832	2.171
C	-1.294	1.896	3.479
H	-1.410	1.005	4.078
H	-4.273	-3.414	4.818
C	-4.531	-2.845	3.916
H	-5.240	-3.444	3.330
H	-5.049	-1.938	4.237
C	-3.318	-2.485	3.124
N	-2.488	-3.424	2.531
H	-2.670	-4.416	2.481
C	-1.465	-2.772	1.918
H	-0.673	-3.251	1.362
N	-1.582	-1.468	2.088
C	-2.733	-1.281	2.831

H	-3.073	-0.293	3.101
H	2.088	-5.233	-0.549
C	1.596	-4.288	-0.294
H	0.541	-4.374	-0.577
H	1.648	-4.163	0.793
C	2.264	-3.123	-1.021
H	3.341	-3.099	-0.818
H	2.175	-3.248	-2.108
C	1.722	-1.733	-0.687
O	0.649	-1.664	0.019
O	2.357	-0.743	-1.124
H	4.167	0.945	5.974
C	4.362	0.641	4.938
H	4.815	1.491	4.420
H	5.104	-0.166	4.951
C	3.108	0.221	4.236
N	2.267	-0.750	4.754
H	2.399	-1.231	5.631
C	1.240	-0.953	3.888
H	0.441	-1.653	4.093
N	1.366	-0.164	2.836
C	2.522	0.571	3.042
H	2.855	1.292	2.310
Mn	-0.145	0.001	1.042
O	-0.232	3.009	-1.866
H	0.065	2.768	-2.758
H	-1.203	2.801	-1.851
O	-1.991	0.444	-0.355
H	-2.240	-0.188	-1.049
H	-2.259	1.315	-0.735
O	1.156	1.346	-0.098
H	1.697	0.643	-0.586
H	0.696	1.889	-0.782